

Influence of inherent and stress-induced anisotropy of hydraulic conductivity on the ground water flow around a rock tunnel

Huang-Kuei Chu, Po-Sung Lai, Jia-Jyun Dong

Graduate Institute of Applied Geology, National Central University, Taiwan (R.O.C.)

(No. 300, Zhongda Rd., Zhongli District, Taoyuan City 32001, Taiwan (R.O.C.)),

Key words; inherent anisotropy, stress-induced anisotropy, tunnel excavating, Oda model, *JRC-JCS* model

Abstract

The hydraulic conductivity around the disposal tunnel is one of the key parameters for the safety assessment of radioactive waste disposal. This study aims to explore the inherent anisotropy (orientation of the discontinuities) and stress induced anisotropy of the hydraulic conductivity around a rock tunnel. *JRC-JCS* model is used to estimate the aperture of discontinuities under stress. Based on the calculated stress field via Kirsch solution and the equivalent continuum model, the hydraulic conductivities around a circular tunnel can be calculated. The groundwater inflow of the tunnel is further evaluated via finite difference method. The result shows that the hydraulic conductivity on the tunnel wall is about 1 ~ 2 orders of magnitude larger than the one away from the tunnel (or the one of rock mass under boundary stress). The major principal hydraulic conductivity on the tunnel wall can be 6 ~ 9 times larger than the minor principal value. The principle directions of the hydraulic conductivity near the tunnel wall are also significantly deviated from the tangential and radial directions when the inherent anisotropy is considered. Groundwater flow analysis shows that the total head and the flow velocity are dominated by the inherent and stress induced anisotropy of hydraulic conductivity. Surprisingly, the inflow of the tunnel is insignificantly influenced by the spatial variation of hydraulic conductivity around the tunnel wall.

1. Introduction

Radioactive waste is usually deposited in rock tunnels. The potential of nuclear species migrating through the rock and the impacts on the biosphere are important issues for tunnel disposal. It is important to assess the permeability of the rock mass around the tunnel for evaluating the groundwater flow field. Due to the presents of primary and secondary discontinuities, rock masses frequently demonstrate inherent anisotropy of hydraulic conductivity. In addition, the stress also affects the aperture of the fissure, which in turn affects the hydraulic conductivity of the rock mass. Therefore, the hydraulic conductivity of rock mass could be anisotropic if the stress tensor is not isotropic.

Oda (1986) proposed a quasi-continuum model to evaluate the hydraulic conductivity of rock mass. The equivalent hydraulic conductivity of rock mass is function of fracture density, persistency, aperture, and orientation of the fractures. Since the aperture of fractures can be evaluated using the stiffness and stresses acting on the fractures, the influences of

inherent anisotropy and stress induced anisotropy can be considered (Cheng, 2006).

In this study, we consider the inherent and stress induced anisotropy of rock mass around the tunnel wall, where the stress redistribution is significant. Finite difference method (FDM) is used to analyze the flow field around the tunnel. To simplify the discussion, the boundary stress is assumed as isotropic. That is, the stress induced anisotropy is only due to stress redistribution caused by tunnel excavation.

2. Hydraulic conductivity around tunnel

The hydraulic conductivity of rock mass is evaluated via Oda model and *JRC-JCS* model, which are briefly introduced below:

(1) Quasi-continuum model

Oda (1985) proposed the concept of fracture tensor, where the fractures of rock mass is assumed as disk shape and the intact rocks are impermeable. The fracture tensor can be expressed as follow Eq. (1):

$$P_{ij} = \frac{\pi \rho}{4} \int_0^{t_m} \int_0^{r_m} \int_{\Omega} r^2 t^3 \hat{n}_i \hat{n}_j E(\hat{n}) f(r) g(t) d\Omega dr dt \quad (1)$$

where ρ is the fracture density, r is the fracture radius, t is the fracture aperture, \hat{n} is the normal vector of fracture. The $E(\hat{n})$, $f(r)$, $g(t)$ are the density function of normal vector, radius and aperture of fractures. The hydraulic conductivity of the fractured rock mass can be expressed as function of fracture density:

$$k_{ij} = \frac{1}{12} (P_{KK} \delta_{ij} - P_{ij}) \quad (2)$$

The inherent anisotropy of hydraulic conductivity is mainly controlled by the density function of normal vector of fractures, and the density function can be approximated by fabric tensor (Kanatani, 1984). In this study, only the second order fabric tensor was considered. The stress induced anisotropy is mainly dominated by the different aperture of fracture with different orientation, which influenced by the stresses acting on the fractures.

(2) JRC-JCS model

Bandis (1982) proposed a JRC-JCS model to evaluate the deformability of discontinuities. The fracture aperture can be obtained if the roughness coefficient JRC_0 and the uniaxial compressive strength JCS_0 (subscript 0 indicates that the test size is 10 cm) are available. The initial aperture (mm) can be calculated using Eq. (3).

$$t_0 = \frac{JRC_0}{5} \left(0.2 \frac{\sigma_c}{JCS_0} - 0.1 \right) \quad (3)$$

σ_c for the intact rock uniaxial compressive strength. If the discontinuity is fresh, then $JCS = \sigma_c$. The maximum closer value of aperture t_{max} comes empirical formula for the regression of test data (Bandis et al., 1983) as follow Eq. (4).

$$t_{max} = -0.3 - 0.006 JRC_0 + 2.24 \left(\frac{JCS_0}{t_0} \right)^{-0.25} \quad (4)$$

Bandis et al. (1983) consider the relationship between normal stress σ_n and the aperture closure Δt , which can be expressed by hyperbolic curve as follows Eq. (5):

$$\Delta t = \frac{\frac{1}{k_0} \sigma_n}{1 + \frac{1}{k_0 t_{max}} \sigma_n} \quad (5)$$

Finally, we can get the aperture (Eq. (6)) cause by normal stress which is function of initial normal stiffness k_0 ($=h/p$, h is constant of normal

stiffness, P is length of discontinuous), normal stress σ_n , roughness coefficient JRC_0 and uniaxial compressive strength JCS_0 .

$$t = t_0 - \Delta t \quad (6)$$

The fracture aperture could be varied under different shear displacement. Based on the fracture shear testing results, Barton (1982) proposed a normalization procedure to evaluate the aperture variation due to shear stress. The JRC_{mob} is roughness coefficient of the discontinuous surface under the action of shear stress, then shear displacement induced normal displacement Δu_n (shear dilatancy) can expressed by the following Eq. (7)

$$\Delta u_n = \delta \tan \left(JRC_{mob} \log \left(\frac{JCS_n}{\sigma_n} \right) \right) \quad (7)$$

$JRC_{mob} \log(JCS_n/\sigma_n)$ is the dilation angle driven by shear stress can be estimated by the single pressure intensity JCS and the normal stress acting on the discontinuous surface.

(3) Mechanical and hydraulic apertures

The aperture t in Eq. (6) is mechanical aperture. However, the aperture in Eq. (1) should be hydraulic aperture, where two parallel plates as the fracture walls were assumed. Based on extensively experimental data, Barton et al. (1985) proposed the empirical relation between the hydraulic aperture e (m) and mechanical aperture E (m) as follows:

$$e = JRC_0^{2.5} / (E/e)^2 \quad (8)$$

JRC_0 is the roughness coefficient for the test size of 100 mm of the discontinuities. Eq. (8) is only applicable to the condition of $E > e$ and this empirical equation is used in this study.

(4) Kirsch's solution

To investigate the influence of the stress anisotropy due to the redistribution of the stress after excavation of the tunnel, Kirsch's solution (Kirsch, 1898) is adopted. Two dimensional stresses around a tunnel can be calculated using Eqs. (9) - (11).

$$\sigma_r = \frac{\sigma_h + \sigma_v}{2} \cdot \left(1 - \frac{a^2}{r^2} \right) + \frac{\sigma_h - \sigma_v}{2} \cdot \left(1 - \frac{4 \cdot a^2}{r^2} + \frac{3 \cdot a^4}{r^4} \right) \cdot \cos 2\theta \quad (9)$$

$$\sigma_\theta = \frac{\sigma_h + \sigma_v}{2} \cdot \left(1 + \frac{a^2}{r^2} \right) - \frac{\sigma_h - \sigma_v}{2} \cdot \left(1 + \frac{3 \cdot a^4}{r^4} \right) \cdot \cos 2\theta \quad (10)$$

$$\tau_{r\theta} = -\frac{\sigma_h - \sigma_v}{2} \cdot \left(1 + \frac{2 \cdot a^2}{r^2} - \frac{3 \cdot a^4}{r^4} \right) \cdot \sin 2\theta \quad (11)$$

In the above equations, σ_r is the radial stress, σ_θ is the tangential stress, $\tau_{r\theta}$ is the shear stress, σ_v and σ_h are the boundary vertical stress and

horizontal stress, a is the tunnel radius and r is the distance from the tunnel center (Fig. 1).

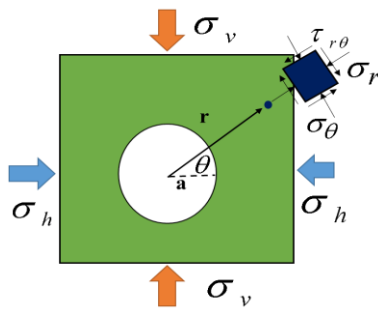


Fig. 1 Schematic diagram of stress after tunnel excavation

The parameters of this study are shown in Table 1. The boundary stress of the tunnel is assumed to be isotropic (the vertical stress equals to the horizontal stress). Radius of the tunnel is 5 meters. Vertical and horizontal effective stresses are 7.5 MPa (about the stress at a depth of 500 m). Two fabric tensors were assumed: (1) isotropic distribution of normal vector ($D_{11} = D_{22} = D_{33} = 0$) and (2) transversely isotropic distribution of normal vector ($D_{11} = D_{22} = -1, D_{33} = 2$).

Table 1 Parameters and conditions used for calculating the hydraulic conductivity

Stress state	Vertical stress σ_v (MPa)	7.5
	Horizontal stress σ_h (MPa)	7.5
Fracture features	Length of discontinuous (m)	1
	JRC of discontinuous (-)	15
	JCS of discontinuous (MPa)	100
	Volume density (strip/m ³)	5
	Discontinuous surface normal vector distribution density function $E(\hat{n}) = 1 + D_{ij}n_i n_j$	
	(a) $D_{11} = D_{22} = 0, D_{33} = 0$	(b) $D_{11} = D_{22} = -1, D_{33} = 2$

The coordinate system adopting by this study is as follows: the axis 1 represents the east, the axis 2 represents the north, the axis 3 represents the upper side and the direction of the tunnel axis (Fig. 2). The tunnel excavation surface of this study will fall on the axis 2 axis 3 plane. The vector can be represented by the space cosine coordinate system (Lee and Farmer, 1993) or in the direction cosine.

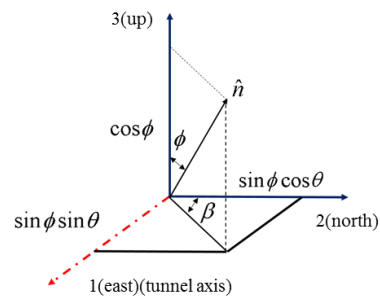


Fig. 2 Schematic diagram of coordinate system

3. Results I- Hydraulic conductivity around tunnel

Fig. 3 shows the principal stresses and principal directions (black cross) of hydraulic conductivity tensor around the tunnel (at distances from the center of the tunnel equal to 1.0, 1.5 and 2.0 times of radius) under an isotropic boundary stress of 7.5 MPa.

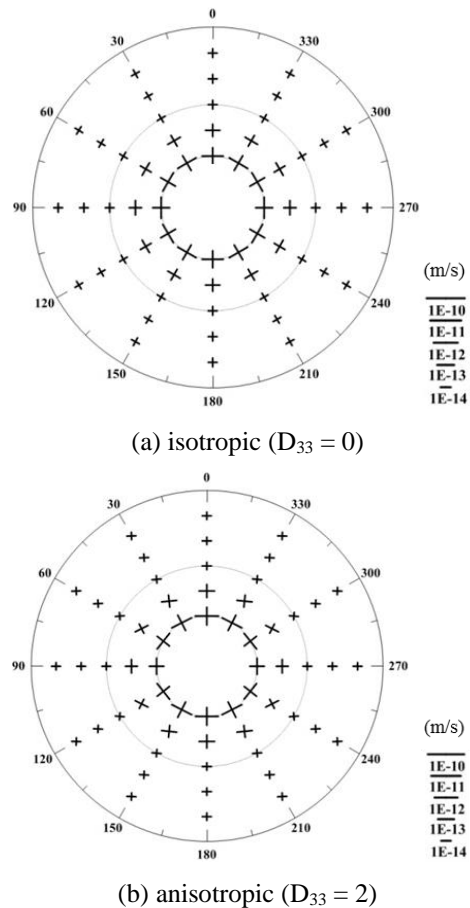
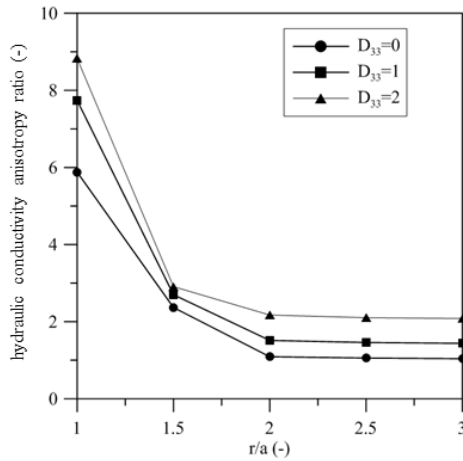


Fig. 3 Distribution of hydraulic conductivity of rock around tunnel

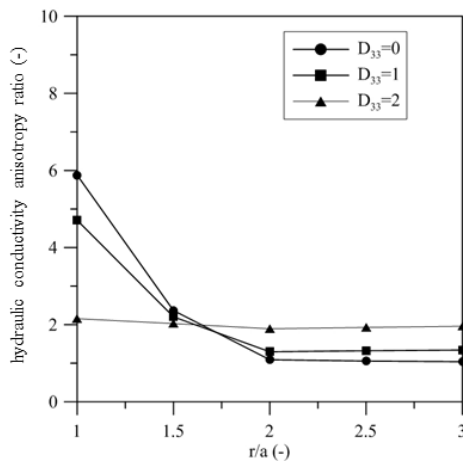
Fig. 3 (a) shows the hydraulic conductivity tensor of an isotropic normal vector distribution ($D_{33} = 0$). The principal directions are in the radial and tangential directions, which is accordance to the principal stress directions. It is indicated that the even the boundary stress and fracture distribution are isotropic, the hydraulic conductivity is anisotropic for

the stress redistribution due to tunnel excavation. The maximum principal direction is in the tangential direction for the fracture parallel to the radial direction tends to close more for larger normal stress than that of the fracture perpendicular the radial direction. The anisotropy reduced when the location away from the tunnel wall for the stress tensor gradually became isotropic. From Fig. 3 (b), the principal directions are no longer in the radial and tangential direction for the anisotropic distribution of the fracture orientation.

Fig. 4 shows the hydraulic conductivity anisotropy ratio (maximum principal value / minimum principal value). When $D_{33} = 0$ (Fig. 4 (a)), the hydraulic conductivity anisotropy ratio equals to 6 times. That is the hydraulic conductivity in tangential direction is 6 times larger than that in radial direction. With increasing distance from the center of the tunnel, the hydraulic conductivity anisotropy reduced rapidly. When $D_{33} = 2$ (Fig. 4 (b)), the anisotropy ratio at the roof of tunnel can be goes up to about 9 (Fig. 4 (a)) while the anisotropic ratio reduced to slightly larger than 2 times at the side wall.



(a) roof of tunnel



(b) side wall of tunnel

Fig. 4 The relationship between the anisotropy ratio of hydraulic conductivity near the tunnel wall

4. Results II- Flow field around tunnel

The flow field around the tunnel was evaluated. The model covers an area of $175 \text{ m} \times 175 \text{ m}$. The tunnel is located in the center of the square and the radius of the tunnel is 5 m. The govern equation of steady-state, two-dimensional groundwater flow can be expressed as:

$$\frac{\partial K_{xx}}{\partial x} \frac{\partial h}{\partial x} + K_{xx} \frac{\partial^2 h}{\partial x^2} + \frac{\partial K_{yy}}{\partial y} \frac{\partial h}{\partial y} + K_{yy} \frac{\partial^2 h}{\partial y^2} + \frac{\partial K_{xy}}{\partial x} \frac{\partial h}{\partial y} + K_{xy} \frac{\partial^2 h}{\partial x \partial y} + \frac{\partial K_{yx}}{\partial y} \frac{\partial h}{\partial x} + K_{yx} \frac{\partial^2 h}{\partial y \partial x} = 0 \quad (11)$$

where the K_{xx} , K_{yy} , K_{xy} , K_{yx} are the four components of hydraulic conductivity tensor. The h is the total head. The finite difference method (FDM) is used to calculate the equal potentials, flow velocity, and flow rate flow into the tunnel. Dirichlet boundary was applied on the outer boundaries of the square. A zero total head was assumed on the inner boundary of the tunnel wall.

The grid is square in shape with a size and $0.5 \text{ m} \times 0.5 \text{ m}$. The stress tensor at each grid was calculated using the Kirsch's solution (Eqs. (9) - (11)) and the hydraulic conductivity can be calculated by Oda's model (Eq. (1)).

Fig. 5 is the flow velocity around the tunnel which the influence of shear dilatancy effect was neglected. The red line segment represents the region with higher flow velocity. The flow direction is in the radial rate around the tunnel is very consistent, and the total flow rate into the tunnel wall is $0.032 \text{ m}^3 / \text{s}$.

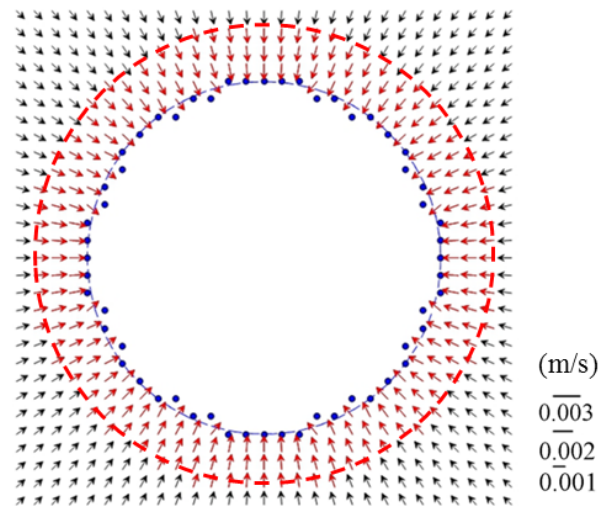


Fig. 5 The flow velocity around the tunnel neglecting the shear dilatancy effect (isotropic ($D_{33} = 0$))

Fig. 6 (a) is the flow velocity around the tunnel which the shear dilatancy effect was considered. The red line segment represents the higher flow rate, which is larger than the average velocity value in this

region. The total flow rate flowing into the tunnel wall is $0.057 \text{ m}^3 / \text{s}$, which is about two times of that when the shear dilatancy was neglected.

Fig. 6 (b) shows the flow velocity around the tunnel for the rock mass with inherent anisotropy. The fabric tensor $D_{33} = 2$. It can be observed that the flow directions are no longer toward to the center of the tunnel for the presence of inherent anisotropy. Generally, the flow velocity is larger at the roof than that at the side wall for the combine effect of normal vector distribution and stress redistribution. The total flow rate flowing into tunnel is $0.054 \text{ m}^3/\text{s}$, which is almost identical to the case for $D_{33} = 0$.

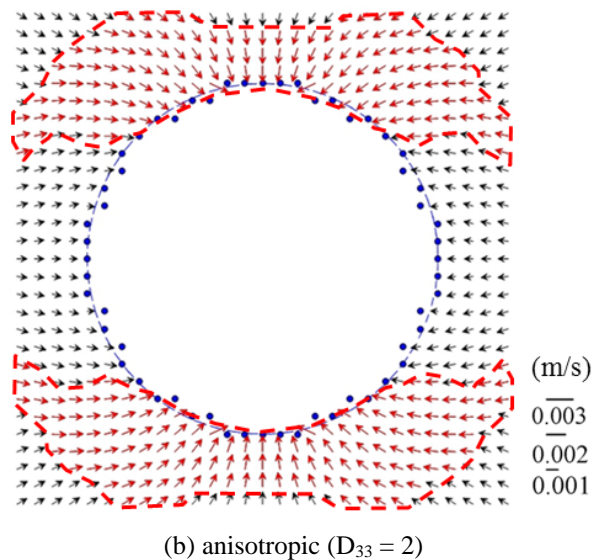
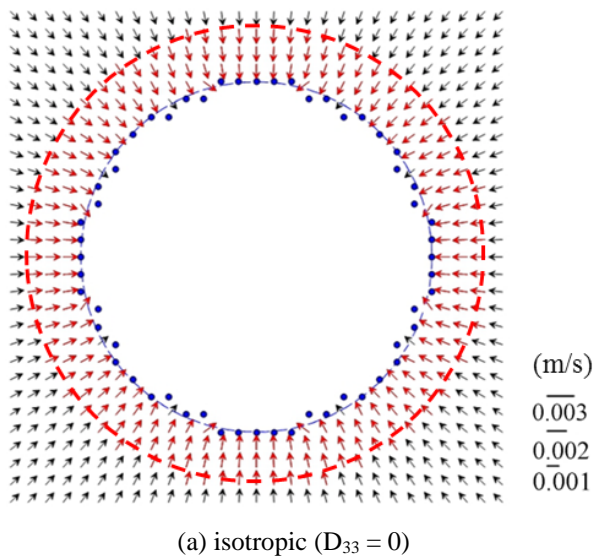


Fig. 6 The flow velocity around the tunnel consider shear dilatancy effect

Fig. 7 (a) shows the equipotential lines (contour lines of total head) around the tunnel with isotropic normal vector distribution ($D_{33}=0$). The equipotential line concentrates the boundary to the tunnel, because

the tunnel excavation caused by the adjacent tunnel wall hydraulic conductivity coefficient increased significantly. This can be seen from the tunnel wall about 0.5 times the radius of the hydraulic gradient slow down.

Fig. 7 (b) shows the equipotential lines (contour lines of total head) around the tunnel with anisotropic normal vector distribution ($D_{33} = 2$). It can be observed that the equipotential lines are elliptical (long axis on horizontal direction). The long axis is passing through the side wall where the hydraulic conductivity is larger than the one on the roof.

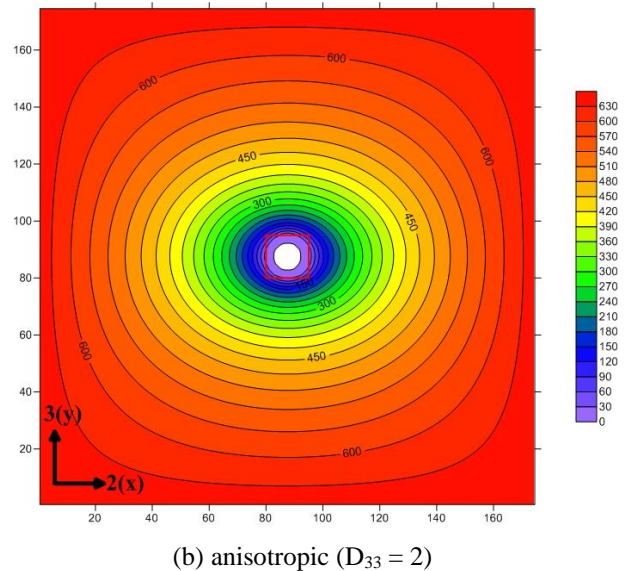
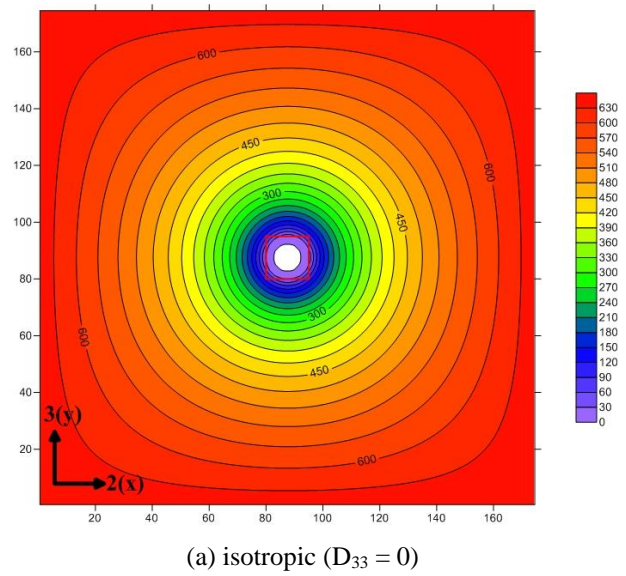


Fig. 7 The equipotential lines around the tunnel

5. Conclusion

Based on the Oda model, the stress-induced anisotropy of hydraulic conductivity caused by the stress redistribution around the tunnel was evaluated. Finite difference method was used to assess the ground water flow around the tunnel. The flow

velocity, equipotential lines, and inflow rate were calculated and the influence of stress-induced and inherent anisotropy of hydraulic conductivity on the flow field was evaluated. Important findings are listed below:

It is found that the redistribution of tunnel excavation stress will obviously change the tensor (principal value, main direction and anisotropy ratio) around the wall of the tunnel and affect the groundwater flow behavior.

1. The hydraulic conductivity around the tunnel increased 1 to 2 orders of magnitude before and after the tunnel excavation, where only the influence of stress redistribution was considered. The influence zone is about one radius of the tunnel.
2. Neglecting shear dilatancy effect significantly underestimates the apertures of fractures and the hydraulic conductivity of rock mass around the tunnel.
3. The hydraulic conductivity tensor (principal values, principal directions and anisotropy ratio) of rock mass around the tunnel is strongly dominated by the anisotropic stress around the tunnel and anisotropic distribution of normal vectors of fractures. If the normal vector distribution is isotropic, the principal directions will be in the radial and tangential directions of the tunnel. However, the principal directions will deviate from the radial and tangential directions if the distribution of normal vector of fractures is anisotropic. When $D_{33} = 2$, the maximum principal value of hydraulic conductivity is 9 times larger than the minimum principal value at tunnel roof.
4. The inflow rate is not significantly influence by the stress redistribution due to tunnel excavation and the normal vector distribution. However, the flow field around the tunnel is significantly affected by the anisotropic hydraulic conductivity, which is influenced by the anisotropic stress field induced by tunnel excavation and the anisotropic distribution of the normal vector of fractures. If the normal vector distribution is isotropic, the flow vectors are toward to the center of the tunnel and the flow velocity is symmetrical. For the case of $D_{33} = 2$, the flow vectors are no longer along the radial directions and the flow velocities at tunnel roof are larger than the ones at side wall.

Reference

- [1] Bandis, S., Lumsden, A. C. and Barton, N. R., Experimental studies of scale effects on the shear behavior of rock joints, *International Journal of Rock Mechanics and Mining Science & Geomechanics Abstracts*, 18 (1), 1-21, 1981.
- [2] Bandis, S., Lumsden, A. C. and Barton, N. R., Fundamentals of rock joint deformation, *International Journal of Rock Mechanics and*

Mining Science & Geomechanics Abstracts, 20 (6), 249-268, 1983.

- [3] Barton, N., Bandis, S. and Bakhtar, K., Strength, deformation and conductivity coupling of rock joints, *International Journal of Rock Mechanics and Mining Science & Geomechanics Abstracts*, 22 (3), 121-140, 1985.
- [4] Knatani, K., Distribution of directional data and fabric tensors. *International Journal of Engineering Science*, 22 (2), 149-164, 1984.
- [5] Lee, C. H., Farmer, I., *Fluid Flow in Discontinuous Rocks..* Chapman and Hall London, 169 pp, 1993.
- [6] Oda, M., Permeability tensor for discontinuous rock masses, *Geotechnique*, 35 (4), 483-495, 1985.
- [7] Oda, M., An equivalent continuum model for coupled stress and fluid flow analysis in jointed rock masses, *Water Resources Research*, 22 (13), 1845-1856, 1986.
- [8] Oda, M., Yamabe, T., Ishizuka, Y., Kumasaka, H., Tada H. and Kimura, K., Elastic stress and strain in jointed rock masses by means of crack tensor analysis, *Rock Mechanics and Rock Engineering*, 26, 89-112, 1993.
- [9] Po-Sung Lai, Inherent and stress-induced anisotropy of hydraulic conductivity around a rock tunnel - equivalent continuum (master's thesis Chinese version), graduate institute of applied geology of National Central University, 2017.
- [10] Yun-Chia Cheng, Inherent and stress-dependent anisotropy of permeability for jointed rock masses (master's thesis Chinese version), graduate institute of applied geology of National Central University, 2006.